HHS Public Access

Author manuscript

Biochim Biophys Acta. Author manuscript; available in PMC 2016 August 01.

Published in final edited form as:

Biochim Biophys Acta. 2015 August ; 1847(8): 681–689. doi:10.1016/j.bbabio.2015.04.004.

Semiquinone Intermediates are involved in the Energy Coupling Mechanism of *E. coli* Complex I

Madhavan Narayanan, **Steven A. Leung**[1], **Yuta Inaba**[1], **Mahmoud M. Elguindy**, and **Eiko Nakamaru-Ogiso**[2]

Johnson Research Foundation, Department of Biochemistry and Biophysics, Perelman School of Medicine, University of Pennsylvania, Philadelphia, PA 19104

Abstract

Complex I (NADH:quinone oxidoreductase) is central to cellular aerobic energy metabolism, and its deficiency is involved in many human mitochondrial diseases. Complex I translocates protons across the membrane using electron transfer energy. Semiquinone (SQ) intermediates appearing during catalysis are suggested to be key for the coupling mechanism in complex I. However, the existence of SQ has remained controversial due to the extreme difficulty in detecting unstable and low intensity SQ signals. Here, for the first time with *E. coli* complex I reconstituted in proteoliposomes, we successfully resolved and characterized three distinct SQ species by EPR. These species include: fast-relaxing SQ (SQ_{Nf}) with $P_{1/2}$ (half-saturation power level) > 50 mW and a wider linewidth (12.8 G); slow-relaxing SQ (SQ_{Ns}) with $P_{1/2}$ = 2–3 mW and a 10 G linewidth; and very slow-relaxing SQ (SQ_{Nvs}) with $P_{1/2}$ = ~ 0.1 mW and a 7.5 G linewidth. The SQ_{Nf} signals completely disappeared in the presence of the uncoupler gramicidin D or squamotacin, a potent *E. coli* complex I inhibitor. The pH dependency of the SQ_{Nf} signals correlated with the proton-pumping activities of complex I. The SQ_{Ns} signals were insensitive to gramicidin D, but sensitive to squamotacin. The SQ_{Nvs} signals were insensitive to both gramicidin D and squamotacin. Our deuterium exchange experiments suggested that SQ_{Nf} is neutral, while SQ_{Ns} and SQ_{Nvs} are anion radicals. The SQ_{Ns} signals were lost in the ΔNuoL mutant missing transporter module subunits NuoL and NuoM. The roles and relationships of the SQ intermediates in the coupling mechanism are discussed.

Keywords

complex I; EPR; semiquinone; iron-sulfur clusters; energy coupling; proton pumping

[2]To whom correspondence should be addressed: to Eiko Nakamaru-Ogiso, Department of Biochemistry and Biophysics, Perelman School of Medicine, University of Pennsylvania, 422 Curie Boulevard, Philadelphia, PA 19104; Tel: (215) 898-5153; Fax: (215) 573-2085; eikoo@mail.med.upenn.edu.

[1]These authors contributed equally to this work.

1. Introduction

Complex I (NADH:quinone oxidoreductase: EC 1.6.5.3) is an entry point for electrons into the respiratory chains of mitochondria and many aerobic organisms. Complex I transfers two electrons from NADH to ubiquione, translocates protons across the membrane, and generates a transmembrane electric potential and proton gradient essential for ATP production and cellular maintenance such as the transport of metabolites and nutrients [1–4]. Electron microscopic analyses indicated that complex I has a characteristic L-shaped structure with two distinct domains; a hydrophilic peripheral arm and a transmembrane hydrophobic arm [5–7]. Now, the three-dimensional X-ray crystal structures confirm the L-shaped structure [8, 9]. While the hydrophilic peripheral domain comprises electron transfer by flavin mononucleotide (FMN) and a chain of seven iron-sulfur (Fe/S) clusters [2], the hydrophobic membrane domain is responsible for proton translocation [10–16] and the binding of quinone and/or specific inhibitors [17–22]. The mechanism of how electron transfer is linked to vectorial proton translocation, however, remains largely unknown. Based on experiments with bovine heart submitochondrial particles (SMP), it is believed that semiquinone (SQ) intermediates appearing during the complex I catalysis are key for the coupling mechanism of electron transfer reactions to transmembrane proton translocation in complex I [23, 24]. Therefore, the understanding of molecular properties and functions of the individual semiquinone species is a prerequisite for elucidating the energy-coupling mechanism of complex I.

There have been several reports on complex I-associated ubisemiquinone EPR signals [23–27]. Tightly coupled submitochondrial particles showed prominent rotenone-sensitive ubisemiquinone signals upon steady-state oxidation of NADH or succinate. The physicochemical properties of these SQ species differ considerably in their spin relaxation behavior. Because SQ species have their spin densities distributed over several atoms, their spin relaxation rates are strongly determined by the neighboring spin systems via spin-spin interactions [28]. Thus, overlapping SQ signals can be resolved based on their relaxation behaviors. Using tightly coupled bovine submitochondrial particles, at least two types of the complex I-associated SQ species were detected by cryogenic EPR [23]: the fast-relaxing ubisemiquinone (SQ_{Nf}) and the slow-relaxing ubisemiquinone (SQ_{Ns}). The SQ_{Nf} signals were seen better in the presence of oligomycin, which was added to increase the respiratory control ratio (RCR) to 7–9. The SQ_{Nf} signals were sensitive to uncouplers, while the SQ_{Ns} signals were insensitive to uncouplers. Both SQ species were equally sensitive to piericidin A, while SQ_{Nf} was ten times more sensitive to rotenone than SQ_{Ns} [23]. These data suggest some differences in their protein microenvironment, favoring the idea that SQ_{Nf} and SQ_{Ns} are different entities accommodated in different quinone binding sites. However, the existence of the second quinone-binding site is currently debated, since the recent X-ray crystal structure has shown only one narrow and long cavity close to the iron-sulfur cluster N2 [9]. Therefore, it is also possible that SQ_{Nf} and SQ_{Ns} can be interpreted as resulting from two mechanistically relevant conformations of a single binding site in the hypothetical two-state stabilization-change mechanism [29].

The detection and isolation of unstable SQ signals in complex I has been very challenging thus far. In intact SMP, there is significant EPR spectral interference from overlapping SQ

signals arising from other respiratory enzyme complexes such as SQ_s in complex II [30, 31] or SQ_i in complex III [31, 32]. In isolated complex I enzymes, only SQ signals attributed to complex I can be detected. Their characteristics, however, would not be the same as those observed in an SMP system *in situ* because there is no membrane potential or proton motive force, and the protein microenvironment surrounding SQ binding sites might be different.

To overcome these problems, we employed a proteoliposome system, which mimics the membrane environment. Until recently, the SQ signals have been characterized only in bovine heart complex I [23, 24], but not yet in bacterial or fungal complex I by EPR. The bacterial complex I catalyzes the same reaction and harbors the same set of cofactors as in bovine heart complex I and consists of only 13–17 subunits [2, 33, 34], of which at least 13–14 have homologs in the mitochondrial enzyme [33]. Because of its simplicity and ease of genetic manipulation, we have chosen *E. coli* complex I as a model system to study the structure and function of complex I. Last year, we established our purification method and obtained highly pure and active complex I from *E. coli* [35]. Using our preparations, we successfully detected SQ signals for the first time in *E. coli* complex I [35]. In the current study, we analyzed SQ signals from purified *E. coli* complex I reconstituted into proteoliposomes by EPR using progressive power saturation and simulation techniques. We improved an algorithm and made a computer program that returned simulated results within minutes and with better accuracy than manual analysis. Using our new program, we compared the biochemical/biophysical profiles of SQ signals between the wild-type and knock-out NuoL (ΔNuoL) mutant. The NuoL subunit is the *E. coli* homolog for mitochondrial ND5, regarded as a transporter module, and it is situated at the distal end of the membrane domain. We report characteristics of these SQ species and discuss their possible functional roles in complex I's electron/proton transfer reaction.

2. Experimental Procedures

2.1 Preparation of the ΔNuoL strain in the $(His)_9$-nuoE MC4100 cells

The $(His)_9$-nuoE cells were generated previously for efficient purification purpose [35]. The NuoL knock-out was generated in this strain by employing the same method described previously [14].

2.2 Isolation of complex I

The *E. coli* complex I was isolated from the wild-type and ΔNuoL strains following the procedure published previously [35]. Briefly, complex I was extracted from the membrane fraction with dodecyl-β-d-maltoside (DDM) at a final concentration of 1.2% (w/v), isolated using Ni-NTA resins, desalted, and concentrated to 3–8 mg protein/ml. The enzyme was quickly frozen in liquid nitrogen and stored at −80 °C until further use.

2.3 Preparation of proteoliposomes

Appropriate amount of Avanti-polar lipid (in chloroform, 25 mg/ml stock) was taken in a clean test-tube and dried first under N_2 and then under vacuum for 4–6 hours. The dried lipid was suspended in a 50 mM Bis-Tris at pH 6.0 buffer containing 50 mM NaCl to a concentration of 8 mg/ml. After the addition of DDM (to a final concentration of 2.5%), the

lipid solution was sonicated until all lipids were dissolved, and the solution became clear. Then, the chilled liposome solution was mixed with complex I in a 4:1 ratio and incubated in a shaker for 5 minutes at 4°C. Immediately, SM2-biobeads were added (50 times the weight of DDM), and the sample mixture was shaken for 3 hours at 4°C. At the end of 3 hours, the sample was washed 5 times with 3 mL of 50 mM Bis-tris pH 6.0 containing 50 mM NaCl buffer to remove biobeads. The collected supernatant was spun down in an ultra-centrifuge for 30 minutes at 150,000 × g. The pellet (proteoliposomes) was dissolved in an appropriate pH buffer. The buffers used in suspension of the proteoliposome pellet were: 5mM MES pH 6.0 containing 50 mM KCl and 2mM $MgCl_2$, 5mM MOPS pH 7.0 containing 50 mM KCl, 5 mM HEPES pH 7.5 containing 50 mM KCl, or 5 mM HEPES pH 8.0 containing 50 mM KCl. The protein concentration of proteoliposome suspensions was measured using Bradford assay and found to be ~ 1.8–2.0 mg/ml. Deuterated proteoliposome was prepared by dissolving the final pellets in 4 mL of freshly prepared 5mM deuterated MOPS pH 7.0 (pD 6.6) buffer containing 50 mM KCl, which was made with 99% D_2O (Sigma) and solid KCl, and the solution pD was adjusted with NaOD (Cambridge Isotope Laboratories) [36]. The suspension was incubated for 30 minutes at 7 °C and was again centrifuged at 150,000 × g for 30 minutes at 7°C. The pellet was immediately suspended in the deuterated MOPS buffer mentioned above. The orientation of the proteoliposomes was determined from the ratio of the specific activities from ferricyanide reductase assay measured in the absence and in the presence of 0.05% DDM [37].

2.4 Proton Translocation Activity

The generation of a proton gradient was determined by monitoring the fluorescence quenching of 9-amino-6-chloro-2-methoxyacridine (ACMA, Sigma). Proteoliposomes (5–20 μL), 0.2 μM ACMA, and 30 μM decylubiquinone (DQ) (Sigma) were added to the assay buffer, 5mM MOPS pH 7.0 containing 50 mM KCl, and incubated at 30 °C for 3–5 min. The fluorescence was detected with a Fluomax-4 spectro-fluorometer (Horiba) at an excitation wavelength of 430 nm and an emission wavelength of 480 nm. The reaction was started by the addition of 50 μM NADH.

2.5 EPR Spectroscopy

EPR samples were prepared under strict anaerobic conditions. Purified complex I samples were reduced with 6 mM NADH or 20 mM neutralized sodium dithionite solution. Reconstituted complex I proteoliposome samples were transferred into EPR tubes, incubated with 400 μM DQ for 15 min. The NADH-DQ oxidoreductase reaction was initiated by the addition of 2 mM NADH, and the mixture was immediately frozen at 10 sec except for the time course experiment. We used a special mixer for mixing samples quickly in EPR tubes, which was previously described [38]. EPR spectra were recorded by a Bruker Elexsys E500 spectrometer at X-band (9.4 GHz) using an Oxford Instrument ESR900 helium flow cryostat. EPR spectra of the semiquinone signals were simulated by Easyspin (http://www.easyspin.org). Simulation of the power saturation curves was performed using MATLAB software (MathWorks Inc), utilizing the trust region reflective algorithm and simplex for non-linear least-square fitting. Power saturation data were analyzed by a fitting method as described previously [24, 39].

2.6 Other analytical procedures

NADH:DQ and NADH:ferricyanide activities in proteoliposomes were spectrophotometrically measured at 30 °C using a Cary 60 UV-visible spectrophotometer (Agilent, Santa Clara, CA). The buffers used were: 5 mM MOPS buffer (pH 7.0) containing 50 mM KCl. Reaction mixtures contained 150 μM NADH and either 30 μM DQ or 1 mM potassium ferricyanide. Extinction coefficients of ε340 = 6.22 mM^{-1} cm−1 for NADH and ε420 = 1.00 mM^{-1} cm^{-1} for ferricyanide were used for activity calculations. Reported values are the average of three measurements. SDS-PAGE and two dimensional SDS-PAGE were performed according to Laemmli [40], Schägger [41], and ref. [42]. The existence of the NuoL and NuoM subunits were immunochemically determined using antibodies specific to NuoL [14] and NuoM [10]. The quantification of bound quinones in purified complex I was performed as described in ref. [35].

3. RESULTS

3.1. Purified complex I from the wild-type and the ΔNuoL variant

To investigate how SQ intermediates are linked to the catalytic reactions, we newly constructed a ΔNuoL mutant strain derived from the $(His)_9$-*nuoE* MC4100 strain for purification. The ΔNuoL complex I has previously been shown to have reduced electron transfer and proton pumping activities [14]. We purified complex I from this strain and from the wild-type. The SDS-PAGE pattern of complex I isolated from the ΔNuoL strain demonstrated the presence of all the subunits NuoA-N except NuoL and NuoM (Fig. 1A). Western blot analysis confirmed that these subunits NuoL and NuoM were below the detection limit in complex I purified from the ΔNuoL strain (Fig. 1B). Because the presence of NuoN in the ΔNuoL complex I was not very clear in the 1D-SDS page (Fig. 1A), we performed two dimensional SDS-PAGE which has been shown to be very effective in separating highly hydrophobic membrane proteins from water soluble proteins such as mitochondrial respiratory chain complexes [42] or synaptic vesicles [43]. By comparing to known patterns of bovine heart complex I [20], we were able to assign the hydrophobic spots as NuoL, NuoM, and NuoN in the wild-type complex I (Fig. 1C). We found that our preparation of the ΔNuoL complex I contained NuoN, but not NuoL and NuoM. Interestingly, the purified ΔNuoL complex I contained 1.11 ± 0.06 moles of ubiquinone per one mole of complex I in contrast to the wild-type which always contained ~2 moles of ubiquinone per one mole of complex I [35]. The representative patterns for proton translocation by the wild-type and ΔNuoL variant after reconstitution in proteoliposomes are shown in Fig. 1D. The proton gradient dissipated after the addition of the uncoupler gramicidin D. The NADH:DQ activity and initial proton pumping rate of the reconstituted ΔNuoL complex I were greatly reduced to ~40% and ~10% of the control, respectively.

3.2. SQ signals in the wild-type and the ΔNuoL complex I

In order to resolve the spectra of multiple SQ signals, we examined the power saturation profiles of the SQ signals at g = 2.004 at 150K using a computer simulation program. Power saturation curves were analyzed by fitting the curves to the equation:

$A=\sum C_i P^{1/2}/(1+P/P_{1/2(\mathrm{i})})0.5b_i$, where A is the amplitude of the total signal observed. C_i

is a coefficient for the actual amplitude of the *i*-th type free radical in the sample, $P_{1/2}(i)$ is the half-saturation power, and b_i is the "inhomogeneity parameter" [39, 44]. A power saturation curve of the signal amplitude was plotted as log signal amplitude divided by square root microwave power *versus* square root microwave power. As shown in Fig. $2A_1$ and $2A_3$, and $2A_2$ and $2A_4$, broad isotropic SQ species were present in both the wild-type and ΔNuoL complex I in their as-isolated form, respectively. As microwave power was increased, the peak-to-peak linewidth (ΔH_{pp}) also increased without changing the center g values. However, after purified complex I was reconstituted into proteoliposomes, three distinct SQ species were detected in the wild-type (Fig. $2B_1$ and $2B_3$): fast-relaxing SQ signals with $P_{1/2}$ (half-saturation power level) = ~50 mW, which is equivalent to SQ_{Nf} reported in bovine heart complex I; slow-relaxing SQ signals with $P_{1/2}$ = ~2 mW, which is equivalent to SQ_{Ns} in bovine heart complex I; and very slow-relaxing SQ signals with $P_{1/2}$ = ~ 0.1 mW, which is possibly equivalent to SQ_{Nx} that was originally reported, but later dismissed as a non- intrinsic complex I component [45]. Therefore, to avoid any possible confusion, in this study, the very slow-relaxing SQ signals were newly designated as SQ_{Nvs} signals. To our surprise, only two SQ species, SQ_{Nf} and SQ_{Nvs} were detected in the ΔNuoL variant (Fig. $2B_2$ and $2B_4$). While the signal amplitude of the SQ_{Nf} species in ΔNuoL decreased to 3.7% of the total signal at 51 mW compared to that in the wild-type (51.9%), the SQ_{Ns} signal was virtually absent in ΔNuoL (only 0.000003% of the total signal at 1 mW), as shown in Fig. $2B_4$. The data clearly suggest that protein-bound SQ signals are extremely sensitive to protein conformation, and that reconstitution into proteoliposomes, which are likely to provide an environment closer to physiological membrane states, is necessary to characterize SQ signals involved in the coupling mechanism. To confirm these power saturation profiles of SQ signals at 150 K, we also analyzed the EPR data obtained at 40 K (Fig. $2C_1$ and $2C_2$). We expected that lower temperatures would slow down relaxation rates of SQ signals, and indeed, the $P_{1/2}$ values for all three SQ signals were drastically decreased (Fig. $2C_3$ and $2C_4$).

Lowering temperatures from 150 K to 40 K did not change the microwave dependence of each SQ species except shifting to lower microwave powers by about one tenth, as seen in Fig. $2B_3$ and $2C_3$ for the wild-type, and Fig. $2B_4$ and $2C_4$ for the ΔNuoL variant. Again, the signal intensity of the SQ_{Ns} (displaying the middle relaxation rate) in the ΔNuoL variant was found to be extremely low (0.09% of the total signalat 0.2 mW) at 40 K (Fig. $2B_4$). However, it became clear that the microwave power dependence patterns of each SQ species were different between the wild-type and ΔNuoL variant at both 150 K and 40 K. This suggests that the protein microenvironment of each SQ species is different between the wild-type and the ΔNuoL variant. The existence of SQ_{Nf} species and the absence of SQ_{Ns} species in the ΔNuoL variant was confirmed at 40K.

3.3. Effect of gramicidin D and squamotacin on SQ species

To characterize SQ species, first, the effects of the uncoupler gramicidin D and the potent *E. coli* complex I inhibitor squamotacin on these three SQ signals were investigated. The fast-relaxing SQ_{Nf} signals completely disappeared in the presence of gramicidin D and in the presence of squamotacin (Fig. 3A). The SQ_{Ns} signals were almost insensitive to gramicidin D, but they were sensitive to squamotacin and the SQ_{Ns} signal intensity decreased to less

than 30% of the control intensity (Fig. 3A). The SQ_{Nvs} signals were insensitive to both gramicidin D and squamotacin (Fig. 3A). These results strongly suggest that the three SQ species distinguished by their relaxation rates indeed have different biochemical properties and are probably localized in different sites in complex I. When substrate NADPH was used, almost no SQ_{Nf} signals (less than 1% of the control intensity with NADH) were observed. However, the signal amplitude of SQ_{Ns} and SQ_{Nvs} increased by 68% and 16%, respectively. Compared to experiments using NADH, SQ_{Ns} became less sensitive to squamotacin, while SQ_{Nvs} increased. The SQ_{Nf} signals in ΔNuoL were also not observed in the presence of gramicidin D, squamotacin, or with NADPH (Fig. 3B). Interestingly, the SQ_{Nvs} signals in ΔNuoL were partially reduced by gramicidin and squamotacin.

3.4. Temperature-dependence of SQ species

In order to investigate the interaction of SQ signals in the wild-type complex I with neighboring paramagnetic species [23], we plotted SQ signal amplitudes as a reciprocal function of temperature in the range from 4 K to 100 K (data not shown). SQ signals detected at 0.01 mW, which contain mostly SQ_{Ns} and SQ_{Nvs}, were inversely proportional to temperature (following the Curie law), indicating that SQ_{Ns} and SQ_{Nvs} components are magnetically isolated from the environment and that their interaction with paramagnetic centers (cluster N2 in this case) is very weak. In contrast, SQ signals detected at 10 mW, which contain all three semiquinone signals, showed weak but some deviation from temperature dependence at very low temperatures (< 10 K). Once SQ_{Nf} signals were abolished by the addition of the uncoupler gramicidin D, this feature almost disappeared in the remaining signals. This suggests a weak magnetic interaction between SQ_{Nf} and cluster N2. However, we did not detect splitting signals due to the magnetic (exchange and dipolar) interactions between SQ_{Nf} and cluster N2, which have previously been reported in tightly coupled bovine SMP [27].

3.5. Simulated EPR spectra of three isolated SQ species

We isolated and simulated individual EPR spectra for these three distinct SQ species observed in the wild-type (Fig. 4). Because at low microwave powers, the slowest SQ_{Nvs} can predominantly be detected, we first chose the EPR data measured at 0.08 mW from the samples treated with squamotacin containing almost no SQ_{Ns} as a representative EPR spectrum for the SQ_{Nvs} species (Fig. 4C). The principal g values were g_z = 2.0061, g_y = 2.0061, and g_x = 2.0051. Then, using these parameters, we obtained a representative EPR spectrum for the SQ_{Ns} species (Fig. 4B) by subtracting the contribution of the SQ_{Nvs} signals based on 2D-power saturation analysis from the EPR data taken from the samples treated with gramicidin D, which contain no SQ_{Nf} at 3 mW. The principal g values for SQ_{Ns} were g_z = 2.0065, g_y = 2.0065, and g_x = 2.0049. Then, the EPR spectrum of the fast-relaxing SQ_{Nf} species was isolated (Fig. 4A) by subtracting the contribution of both SQ_{Ns} and SQ_{Nvs} from the EPR data measured at 20 mW. The peak-to-peak linewidths (ΔH_{pp}) for SQ_{Nf}, SQ_{Ns}, and SQ_{Nvs} were 12.8 G, 10 G, and 7.5 G, respectively. Our data are consistent with the characteristics of bovine counterparts for which SQ_{Nf} has a wider linewidth (8.4 G) [27] than SQ_{Ns} (7.0 G) [45]. Interestingly, in addition to the difference in their linewidths, the spectral line shape was also very different among those SQ species. The Gaussian and Lorentzian broadening ratios for SQ_{Nf}, SQ_{Ns}, and SQ_{Nvs} were 1 to 0, 0.75 to 0.25, and 0 to

1, respectively, indicating that SQ_{Nf} is confined in a dense environment surrounded by amino acid side chains while SQ_{Nvs} is localized in a free environment, probably close to the outside of the protein [46]. Under strict anaerobic conditions, the total spin concentration of the SQ signals detected in our system was estimated as ~2.2% per complex I. The ratio among these three SQ signal intensities was dependent on the microwave power. In the 10 sec (after the addition of NADH) samples, we typically obtained SQ_{Nf} : SQ_{Ns} : SQ_{Nvs} = 0.62 : 0.28 : 0.1 at 10 mW. So, roughly, SQ_{Nf}, SQ_{Ns}, and SQ_{Nvs} were 1.36%, 0.62%, and 0.22% per complex I.

3.6 Time course

We examined the generation and decay time course for these three SQ species as shown in Fig. 5. The reaction was started with 2 mM NADH, and the reaction mixture was frozen at time points of 0 s, 5 s, 10 s, and 60 s. We found that the SQ_{Ns} and SQ_{Nvs} signal intensities reached their maximum levels at 5 s (red and green bars in Fig. 5) while the SQ_{Nf} signal intensity peaked at 10 s (blue bar in Fig. 5). As for the decay speed, SQ_{Nf} was the fastest, and SQ_{Ns} was the slowest. This supports the possibility that these three SQ signals are distinct entities. The signal amplitude at 0 sec was determined from the EPR data for the sample in which only DQ was added (no NADH). We detected a relatively high intensity of SQ_{Nf} at 0 sec, which might result from fast-relaxing SQ species in a free Q pool environment due to a high concentration of DQ (400 uM) in the sample at 0 sec. These non-protein bound SQ species are known to be very fast relaxating [47], thus, they are not distinguishable from the protein-bound SQ_{Nf} signal by power saturation analysis.

3.7 pH Dependence of SQ species

Fig. 6A shows the pH dependency of these three SQ signals in the wild-type. As pH was raised above 7, the SQ_{Nf} signal intensity decreased. The SQ_{Nf} signal intensity at pH 8, for example, decreased to one tenth of the amplitude at pH 7. In stark contrast, the SQ_{Ns} and SQ_{Nvs} signal intensities significantly increased as pH increased. The pH dependency of the SQ_{Nf} signals correlated with the proton-pumping activities at pH 7 and above (Fig. 6B) and with NADH:DQ activities (data not shown). We observed much lower proton pumping activities at pH 6, although the SQ_{Nf} signal intensity was nearly as high as that observed at pH 7. This pH dependence profile of SQ_{Nf} was similar to that of SQ_{Nf} observed in bovine SMP [27].

3.8 Deuterium effect on SQ species

It is known that protonation increases spectral linewidth because of an asymmetric perturbation of the spin density on the quinone ring [31, 48]. According to previous literatures, the linewidths of neutral ubisemiquinones are always much larger (~12 G) than those of the corresponding anion radicals (7–9 G). Therefore, the wider linewidth (12.8 G) of the SQ_{Nf} signal suggests that the SQ_{Nf} species could be in a neutral form (QH•). To investigate this possibility, we prepared proteoliposomes in a deuterated buffer. As expected based on previous studies [49–51], the peak-to peak linewidth decreased to 10.2 G (Fig. 7A), indicating that SQ_{Nf} could be a neutral semiquinone radical. No difference was observed in the linewidths of SQ_{Ns} and SQ_{Nvs} (data not shown), relaxation profiles of three SQ species (Fig. 7B), or the gramicidin D responsiveness of three SQ species (data not

shown). However, the NADH:DQ activity and initial proton pumping rate in the deuterated complex I proteoliposomes were greatly reduced to ~50% and ~40% of the control, respectively (data not shown).

4 DISCUSSION

In this study, for the first time, we successfully detected and characterized the distinct molecular properties of three SQ signals resolved by their different spin-relaxation behaviors in purified *E. coli* complex I reconstituted in proteoliposomes. Two of them, SQ_{Nf} and SQ_{Ns} are equivalent to the SQ species that have been observed in bovine heart SMP. We confirmed previously described, important features like the presence of SQ_{Nf} is dependent on the membrane potential and its complete disappearance with the addition of uncouplers, while SQ_{Ns} is insensitive to uncouplers [23, 27]. The differences in their sensitivities to the potent *E. coli* complex I inhibitor squamotacin is also very similar to that observed with rotenone in bovine SMP [52]. In this study, we further revealed new details regarding SQ_{Nf} and $SQ_{Ns.}$

One of our most important findings is that there was no SQ_{Ns} signal in the ΔNuoL mutant, while the SQ_{Nf} signal was still detectable. This ΔNuoL mutant showed only ~10% of the control's proton pumping activities, although the electron transfer activity (NADH-DQ) was ~40% of the wild-type. This suggests a lower proton pumping ratio in this variant. Although SQ_{Ns} was previously suggested to be remotely located from cluster N2 (estimated > 30 Å) [23], the location of SQ_{Ns} is unknown. Plus, it is not clear why the ΔNuoL variant, which contains up to NuoN that extends 100Å away from the primary catalytic site, contains only one bound quinone, while the wild-type complex I contain two bound quinones per complex I. Further studies are required to elucidate how the loss of the secondary bound Q is related to the disappearance of SQ_{Ns} in ΔNuoL. At least, it is reasonable to conclude that SQ_{Ns} plays a critical role for the proton pumping mechanism of complex I.

Our other important finding is that the SQ_{Nf} species in *E. coli* complex I is seemingly protonated, in contrast to the SQ_{Nf} species in bovine heart complex I, which was found to be anionic [27]. The highly conserved Tyr84 in the NuoD subunit of complex I is only ~ 7 Å away from cluster N2, and it faces the quinone binding site based on the crystal structures of *Thermus thermophilus* complex I [9, 53]. Mutational analyses of the corresponding residue Tyr144 in *Yarrowia lipolytica* revealed that this residue is essential for complex I activities in both electron and proton transfer [54]. Therefore, it is likely that this Tyr84 residue (and/or possibly Glu83) could be a proton donor for the enzyme's SQ_{Nf}.

SQ_{Nf} is the direct electron acceptor from cluster N2 with an estimated distance of 12 Å [27], which was calculated based on a strong magnetic interaction between cluster N2 and SQ_{Nf} observed in bovine SMP. Our results including the extremely high sensitivities to uncouplers and inhibitors, and the pH dependency of the SQ_{Nf} signals correlating with the proton-pumping activities of complex I, support the possibility that the SQ_{Nf} is directly involved in proton pumping activities. According to the recent crystal structures of the entire *T. thermophilus* complex I with the quinone analogues piericidin A (a complex I inhibitor) and DQ, "the quinone-reaction chamber" (equivalent to the SQ_{Nf} binding site) is unusually long,

narrow and enclosed [9]. The 100% Gaussian broadening feature (Fig. 4A) also supports the conclusion that SQ_{Nf} is located deeply in a dense environment interacting with amino acid side chains such that it could trigger conformational changes in proton transfer subunits.

Based on several features of SQ_{Ns} such as the 75% Gaussian broadening features (Fig. 4B) which suggests that SQ_{Ns} is largely surrounded by protein environment, complex I inhibitor sensitiveness, the generation of SQ_{Ns} by NADPH, and the absence of SQ_{Ns} signals in ΔNuoL, it is likely that SQ_{Ns} could be linked to the catalytic site through an unknown mechanism. Also, SQ_{Ns} seems to have a role for stabilizing the SQ_{Nf} generation during the complex I catalysis. We previously reported that when ND5 (bovine homolog of NuoL) was labeled with a photoaffinity analog of the potent complex I inhibitor fenpyroxymate, the labeling was in parallel with inhibition of NADH oxidase activity [18]. Furthermore, the ND5 labeling was completely prevented by various complex I inhibitors [18]. At present, it is a mystery how this photoaffinity-labeled possible second Q binding site in ND5 is related to the loss of the secondary bound Q in the isolated ΔNuoL complex I.

Regarding SQ_{Nvs}, its insensitivity to squamotacin and the 100% Lorentzian broadening features (Fig. 4C) suggest that it is in a free environment likely very close to the Q pool. But SQ_{Nvs} is still a legitimate complex I-associated SQ species, since it appears after the addition of NADH and disappears faster than SQ_{Ns} as NADH is consumed. The role of SQ_{Nvs} in the complex I catalytic mechanism is totally unknown at this moment, however, it was reported in a study of steady state kinetics that the rotenone-insensitive reaction in bovine complex I is also physiologically relevant [55]. The SQ_{Nvs} might be involved in this complex I inhibitor insensitive reaction. It is tempting to speculate that this site is in a dynamic equilibrium with the Q pool in the membrane and provides a route to release some electrons under certain conditions when complex I receives electrons exceeding its capacity at the SQ_{Nf} binding site.

One of our surprising results was that the characteristics of SQ signals observed from as-isolated complex I were completely different from those observed from complex I that was reconstituted into proteoliposomes, which provide closer to physiological conditions. We saw mostly one major isotopic SQ species in both the isolated wild-type and ΔNuoL complex I. The distinct profiles of three SQ signals and their differences in SQ signals between the wild-type and ΔNuoL complex I were not detected until the proteins were reconstituted into proteoliposomes (Fig. 2B). On the other hand, the main features of the SQ_{Ns} signals were still observed in as-isolated bovine complex I under aerobic conditions [45]. This could be due to the SQ binding sites in bovine complex I being well shielded from the outside with many supernumerary subunits. The spin concentration of the total SQ signals detected in our system was estimated as ~2.2% per complex I under anaerobic conditions. The *E. coli* SQ binding sites are probably more exposed to the outside, thus, SQ signals are much more unstable. Therefore, it is reasonable that no SQ signals in isolated *E. coli* complex I were observed under aerobic conditions by EPR previously [56].

In conclusion, we successfully detected and characterized three semiquinone intermediates in *E. coli* complex I during turnover. Our present results strongly suggest that both SQ_{Nf} and SQ_{Ns} are involved in the energy coupling mechanism of complex I.

Acknowledgments

This work was supported by NIH grant RO1GM097409 to E.N.-O. and AHA grant 11SDG5560001 to E.N.-O.

The abbreviations used are

DDM	dodecyl-β-D-maltoside
DQ	decylubiquinone
MK	menaquinone
Q	quinone
SMP	submitochondrial particles
SQ	semiquinone
UQ	ubiquinone

References

1. Yagi T, Matsuno-Yagi A. The proton-translocating NADH-quinone oxidoreductase in the respiratory chain: the secret unlocked. Biochemistry. 2003; 42:2266–2274. [PubMed: 12600193]
2. Sazanov LA. Respiratory complex I: mechanistic and structural insights provided by the crystal structure of the hydrophilic domain. Biochemistry. 2007; 46:2275–2288. [PubMed: 17274631]
3. Brandt U. Energy converting NADH:quinone oxidoreductase (complex I). Annu Rev Biochem. 2006; 75:69–92. [PubMed: 16756485]
4. Hirst J. Mitochondrial complex I. Annu Rev Biochem. 2013; 82:551–575. [PubMed: 23527692]
5. Hofhaus G, Weiss H, Leonard K. Electron microscopic analysis of the peripheral and membrane parts of mitochondrial NADH dehydrogenase (complex I). J Mol Biol. 1991; 221:1027–1043. [PubMed: 1834851]
6. Vinothkumar KR, Zhu J, Hirst J. Architecture of mammalian respiratory complex I. Nature. 2014; 515:80–84. [PubMed: 25209663]
7. Clason T, Ruiz T, Schagger H, Peng G, Zickermann V, Brandt U, Michel H, Radermacher M. The structure of eukaryotic and prokaryotic complex I. J Struct Biol. 2010; 169:81–88. [PubMed: 19732833]
8. Hunte C, Zickermann V, Brandt U. Functional modules and structural basis of conformational coupling in mitochondrial complex I. Science. 2010; 329:448–451. [PubMed: 20595580]
9. Baradaran R, Berrisford JM, Minhas GS, Sazanov LA. Crystal structure of the entire respiratory complex I. Nature. 2013; 494:443–448. [PubMed: 23417064]
10. Torres-Bacete J, Nakamaru-Ogiso E, Matsuno-Yagi A, Yagi T. Characterization of the NuoM (ND4) subunit in Escherichia coli NDH-1: conserved charged residues essential for energy-coupled activities. J Biol Chem. 2007; 282:36914–36922. [PubMed: 17977822]
11. Kao MC, Di Bernardo S, Perego M, Nakamaru-Ogiso E, Matsuno-Yagi A, Yagi T. Functional roles of four conserved charged residues in the membrane domain subunit NuoA of the proton-translocating NADH-quinone oxidoreductase from Escherichia coli. J Biol Chem. 2004; 279:32360–32366. [PubMed: 15175326]
12. Kao MC, Nakamaru-Ogiso E, Matsuno-Yagi A, Yagi T. Characterization of the membrane domain subunit NuoK (ND4L) of the NADH-quinone oxidoreductase from Escherichia coli. Biochemistry. 2005; 44:9545–9554. [PubMed: 15996109]
13. Kao MC, Di Bernardo S, Nakamaru-Ogiso E, Miyoshi H, Matsuno-Yagi A, Yagi T. Characterization of the membrane domain subunit NuoJ (ND6) of the NADH-quinone oxidoreductase from Escherichia coli by chromosomal DNA manipulation. Biochemistry. 2005; 44:3562–3571. [PubMed: 15736965]

14. Nakamaru-Ogiso E, Kao MC, Chen H, Sinha SC, Yagi T, Ohnishi T. The membrane subunit NuoL(ND5) is involved in the indirect proton pumping mechanism of Escherichia coli complex I. J Biol Chem. 2010; 285:39070–39078. [PubMed: 20826797]
15. Amarneh B, Vik SB. Mutagenesis of subunit N of the Escherichia coli complex I. Identification of the initiation codon and the sensitivity of mutants to decylubiquinone. Biochemistry. 2003; 42:4800–4808. [PubMed: 12718520]
16. Sato M, Sinha PK, Torres-Bacete J, Matsuno-Yagi A, Yagi T. Energy transducing roles of antiporter-like subunits in Escherichia coli NDH-1 with main focus on subunit NuoN (ND2). J Biol Chem. 2013; 288:24705–24716. [PubMed: 23864658]
17. Murai M, Ishihara A, Nishioka T, Yagi T, Miyoshi H. The ND1 subunit constructs the inhibitor binding domain in bovine heart mitochondrial complex I. Biochemistry. 2007; 46:6409–6416. [PubMed: 17474759]
18. Nakamaru-Ogiso E, Sakamoto K, Matsuno-Yagi A, Miyoshi H, Yagi T. The ND5 subunit was labeled by a photoaffinity analogue of fenpyroximate in bovine mitochondrial complex I. Biochemistry. 2003; 42:746–754. [PubMed: 12534287]
19. Yagi T, Hatefi Y. Identification of the dicyclohexylcarbodiimide-binding subunit of NADH-ubiquinone oxidoreductase (Complex I). J Biol Chem. 1988; 263:16150–16155. [PubMed: 3141400]
20. Nakamaru-Ogiso E, Han H, Matsuno-Yagi A, Keinan E, Sinha SC, Yagi T, Ohnishi T. The ND2 subunit is labeled by a photoaffinity analogue of asimicin, a potent complex I inhibitor. FEBS Lett. 2010; 584:883–888. [PubMed: 20074573]
21. Tocilescu MA, Zickermann V, Zwicker K, Brandt U. Quinone binding and reduction by respiratory complex I. Biochim Biophys Acta. 2010; 1797:1883–1890. [PubMed: 20493164]
22. Shiraishi Y, Murai M, Sakiyama N, Ifuku K, Miyoshi H. Fenpyroximate binds to the interface between PSST and 49 kDa subunits in mitochondrial NADH-ubiquinone oxidoreductase. Biochemistry. 2012; 51:1953–1963. [PubMed: 22353032]
23. Magnitsky S, Toulokhonova L, Yano T, Sled VD, Hagerhall C, Grivennikova VG, Burbaev DS, Vinogradov AD, Ohnishi T. EPR characterization of ubisemiquinones and iron-sulfur cluster N2, central components of the energy coupling in the NADH-ubiquinone oxidoreductase (complex I) in situ. J Bioenerg Biomembr. 2002; 34:193–208. [PubMed: 12171069]
24. Vinogradov AD, Sled VD, Burbaev DS, Grivennikova VG, Moroz IA, Ohnishi T. Energy-dependent Complex I-associated ubisemiquinones in submitochondrial particles. FEBS Lett. 1995; 370:83–87. [PubMed: 7649309]
25. Suzuki H, King TE. Evidence of an ubisemiquinone radical(s) from the NADH-ubiquinone reductase of the mitochondrial respiratory chain. J Biol Chem. 1983; 258:352–358. [PubMed: 6294105]
26. De Jong AM, Albracht SP. Ubisemiquinones as obligatory intermediates in the electron transfer from NADH to ubiquinone. Eur J Biochem. 1994; 222:975–982. [PubMed: 8026508]
27. Yano T, Dunham WR, Ohnishi T. Characterization of the delta muH+-sensitive ubisemiquinone species (SQ(Nf)) and the interaction with cluster N2: new insight into the energy-coupled electron transfer in complex I. Biochemistry. 2005; 44:1744–1754. [PubMed: 15683258]
28. Grimaldi S, Ostermann T, Weiden N, Mogi T, Miyoshi H, Ludwig B, Michel H, Prisner TF, MacMillan F. Asymmetric binding of the high-affinity Q(H)(*)(−) ubisemiquinone in quinol oxidase (bo3) from Escherichia coli studied by multifrequency electron paramagnetic resonance spectroscopy. Biochemistry. 2003; 42:5632–5639. [PubMed: 12741819]
29. Brandt U. A two-state stabilization-change mechanism for proton-pumping complex I. Biochim Biophys Acta. 2011; 1807:1364–1369. [PubMed: 21565159]
30. Miki T, Yu L, Yu CA. Characterization of ubisemiquinone radicals in succinate-ubiquinone reductase. Arch Biochem Biophys. 1992; 293:61–66. [PubMed: 1309986]
31. JRaO; Bowyer, T. EPR spedtrostudy in the study of ubisemiquinones in redox chains. In: Lenaz, G., editor. Coenxyme Q. John Wiley & Sons; New York: 1985. p. 409-432.
32. Meinhardt SW, Yang XH, Trumpower BL, Ohnishi T. Identification of a stable ubisemiquinone and characterization of the effects of ubiquinone oxidation-reduction status on the Rieske iron-

sulfur protein in the three-subunit ubiquinol-cytochrome c oxidoreductase complex of Paracoccus denitrificans. J Biol Chem. 1987; 262:8702–8706. [PubMed: 3036822]

33. Yagi T, Yano T, Di Bernardo S, Matsuno-Yagi A. Procaryotic complex I (NDH-1), an overview. Biochim Biophys Acta. 1998; 1364:125–133. [PubMed: 9593856]
34. Yip CY, Harbour ME, Jayawardena K, Fearnley IM, Sazanov LA. Evolution of respiratory complex I: "supernumerary" subunits are present in the alpha-proteobacterial enzyme. J Biol Chem. 286:5023–5033. [PubMed: 21115482]
35. Narayanan M, Gabrieli DJ, Leung SA, Elguindy MM, Glaser CA, Saju N, Sinha SC, Nakamaru-Ogiso E. Semiquinone and cluster N6 signals in His-tagged proton-translocating NADH:ubiquinone oxidoreductase (complex I) from Escherichia coli. J Biol Chem. 2013; 288:14310–14319. [PubMed: 23543743]
36. Huyghues-Despointes BM, Pace CN, Englander SW, Scholtz JM. Measuring the conformational stability of a protein by hydrogen exchange. Methods Mol Biol. 2001; 168:69–92. [PubMed: 11357629]
37. Stolpe S, Friedrich T. The Escherichia coli NADH:ubiquinone oxidoreductase (complex I) is a primary proton pump but may be capable of secondary sodium antiport. J Biol Chem. 2004; 279:18377–18383. [PubMed: 14970214]
38. Ohnishi ST, Shinzawa-Itoh K, Ohta K, Yoshikawa S, Ohnishi T. New insights into the superoxide generation sites in bovine heart NADH-ubiquinone oxidoreductase (Complex I): the significance of protein-associated ubiquinone and the dynamic shifting of generation sites between semiflavin and semiquinone radicals. Biochim Biophys Acta. 2010; 1797:1901–1909. [PubMed: 20513438]
39. Rupp H, Rao KK, Hall DO, Cammack R. Electron spin relaxation of iron-sulphur proteins studied by microwave power saturation. Biochim Biophys Acta. 1978; 537:255–260. [PubMed: 215217]
40. Laemmli UK. Cleavage of structural proteins during the assembly of the head of bacteriophage T4. Nature. 1970; 227:680–685. [PubMed: 5432063]
41. Schagger H. Tricine-SDS-PAGE. Nat Protoc. 2006; 1:16–22. [PubMed: 17406207]
42. Rais I, Karas M, Schagger H. Two-dimensional electrophoresis for the isolation of integral membrane proteins and mass spectrometric identification. Proteomics. 2004; 4:2567–2571. [PubMed: 15352231]
43. Burre J, Beckhaus T, Schagger H, Corvey C, Hofmann S, Karas M, Zimmermann H, Volknandt W. Analysis of the synaptic vesicle proteome using three gel-based protein separation techniques. Proteomics. 2006; 6:6250–6262. [PubMed: 17080482]
44. Beinert, H.; Orne-Johnson, W. Electron Spin Relaxation as a probe for active centers of paramagnetic enzyme species. In: Ehrenberg, A.; Malmstrom, BG.; Vanngard, T., editors. Magnetic Resonance in Biological Systems. Pergamon Press; New York: 1967. p. 221-247.
45. Ohnishi T, Johnson JE Jr, Yano T, Lobrutto R, Widger WR. Thermodynamic and EPR studies of slowly relaxing ubisemiquinone species in the isolated bovine heart complex I. FEBS Lett. 2005; 579:500–506. [PubMed: 15642366]
46. Bales BL, Peric M, Lamy-Freund MT. Contributions to the Gaussian line broadening of the proxyl spin probe EPR spectrum due to magnetic-field modulation and unresolved proton hyperfine structure. J Magn Reson. 1998; 132:279–286. [PubMed: 9632554]
47. Ingledew WJ, Ohnishi T, Salerno JC. Studies on a stabilisation of ubisemiquinone by Escherichia coli quinol oxidase, cytochrome bo. Eur J Biochem. 1995; 227:903–908. [PubMed: 7867653]
48. Hales BJ, Case EE. Immobilized radicals IV. Biological semiquinone anions and neutral semiquinones. Biochim Biophys Acta. 1981; 637:291–302.
49. Kay CW, Feicht R, Schulz K, Sadewater P, Sancar A, Bacher A, Mobius K, Richter G, Weber S. EPR, ENDOR, and TRIPLE resonance spectroscopy on the neutral flavin radical in Escherichia coli DNA photolyase. Biochemistry. 1999; 38:16740–16748. [PubMed: 10606505]
50. Dikanov SA, Samoilova RI, Kolling DR, Holland JT, Crofts AR. Hydrogen bonds involved in binding the Qi-site semiquinone in the bc1 complex, identified through deuterium exchange using pulsed EPR. J Biol Chem. 2004; 279:15814–15823. [PubMed: 14736869]
51. Klughammer C, Klughammer B, Pace R. Deuteration effects on the in vivo EPR spectrum of the reduced secondary photosystem I electron acceptor A1 in cyanobacteria. Biochemistry. 1999; 38:3726–3732. [PubMed: 10090761]

52. Ohnishi T, Ohnishi ST, Shinzawa-Itoh K, Yoshikawa S, Weber RT. EPR detection of two protein-associated ubiquinone components (SQ(Nf) and SQ(Ns)) in the membrane in situ and in proteoliposomes of isolated bovine heart complex I. Biochim Biophys Acta. 2012; 1817:1803–1809. [PubMed: 22503829]

53. Sazanov LA, Hinchliffe P. Structure of the hydrophilic domain of respiratory complex I from Thermus thermophilus. Science. 2006; 311:1430–1436. [PubMed: 16469879]

54. Tocilescu MA, Fendel U, Zwicker K, Drose S, Kerscher S, Brandt U. The role of a conserved tyrosine in the 49-kDa subunit of complex I for ubiquinone binding and reduction. Biochim Biophys Acta. 2010; 1797:625–632. [PubMed: 20117074]

55. Nakashima Y, Shinzawa-Itoh K, Watanabe K, Naoki K, Hano N, Yoshikawa S. The second coenzyme Q1 binding site of bovine heart NADH: coenzyme Q oxidoreductase. J Bioenerg Biomembr. 2002; 34:89–94. [PubMed: 12018892]

56. Verkhovskaya ML, Belevich N, Euro L, Wikstrom M, Verkhovsky MI. Real-time electron transfer in respiratory complex I. Proc Natl Acad Sci U S A. 2008; 105:3763–3767. [PubMed: 18316732]

Highlights

- Three semiquinone species in *E. coli* complex I are resolved by EPR analysis.
- Biochemical/biophysical features of each semiquinone species are studied.
- We compare semiquinone features between the wild-type and the ΔNuoL mutant.
- The fast relaxing SQ_{Nf} and slow relaxing SQ_{Ns} are likely involved in energy coupling.

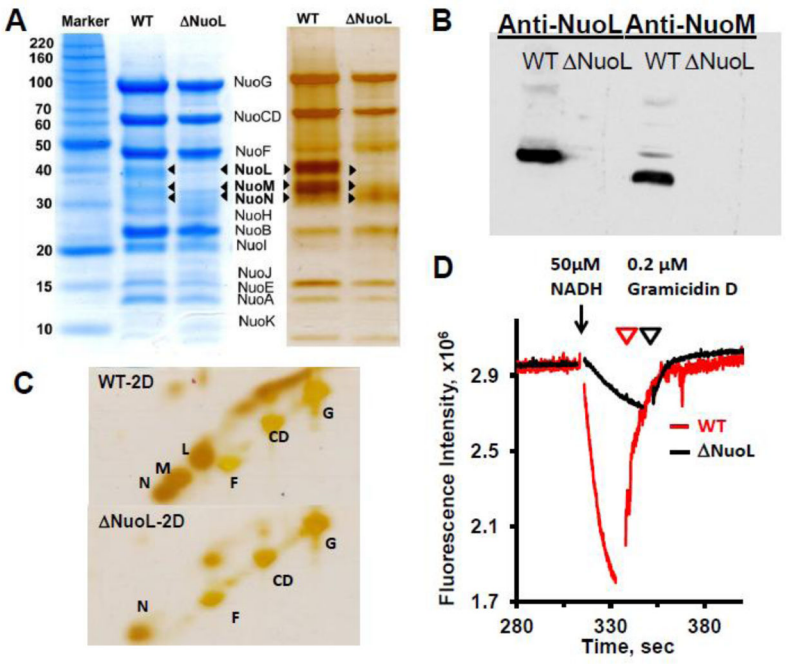

Fig. 1.

SDS-PAGE analyses of purified complex I from the wild-type and the ΔNuoL variant, and their proton translocation activities after reconstitution into proteoliposomes. (A) 1D Tricine SDS-PAGE stained with Coomassie Brilliant Blue (*left*) and silver (*right*). (B) Immunoblotting with anti-NuoL and anti-NuoM antibodies. (C) Two dimensional SDS analysis. (D) Generation of a proton gradient monitored by the quench of the ACMA fluorescence. The NADH-DQ and NADH:ferricyanide activities were 12.23 and 58.58, 5.15, and 137.63 μmol/min/mg for the WT and ΔNuoL preparations, respectively. The data were normalized based on the complex I concentrations of the wild-type (MW 537 kDa) and the ΔNuoL variant (MW 417 kDa, lacking NuoL and NuoM) and the complex I orientation factor in the proteoliposomes (79% for the wild-type; 62% for the ΔNuoL variant).

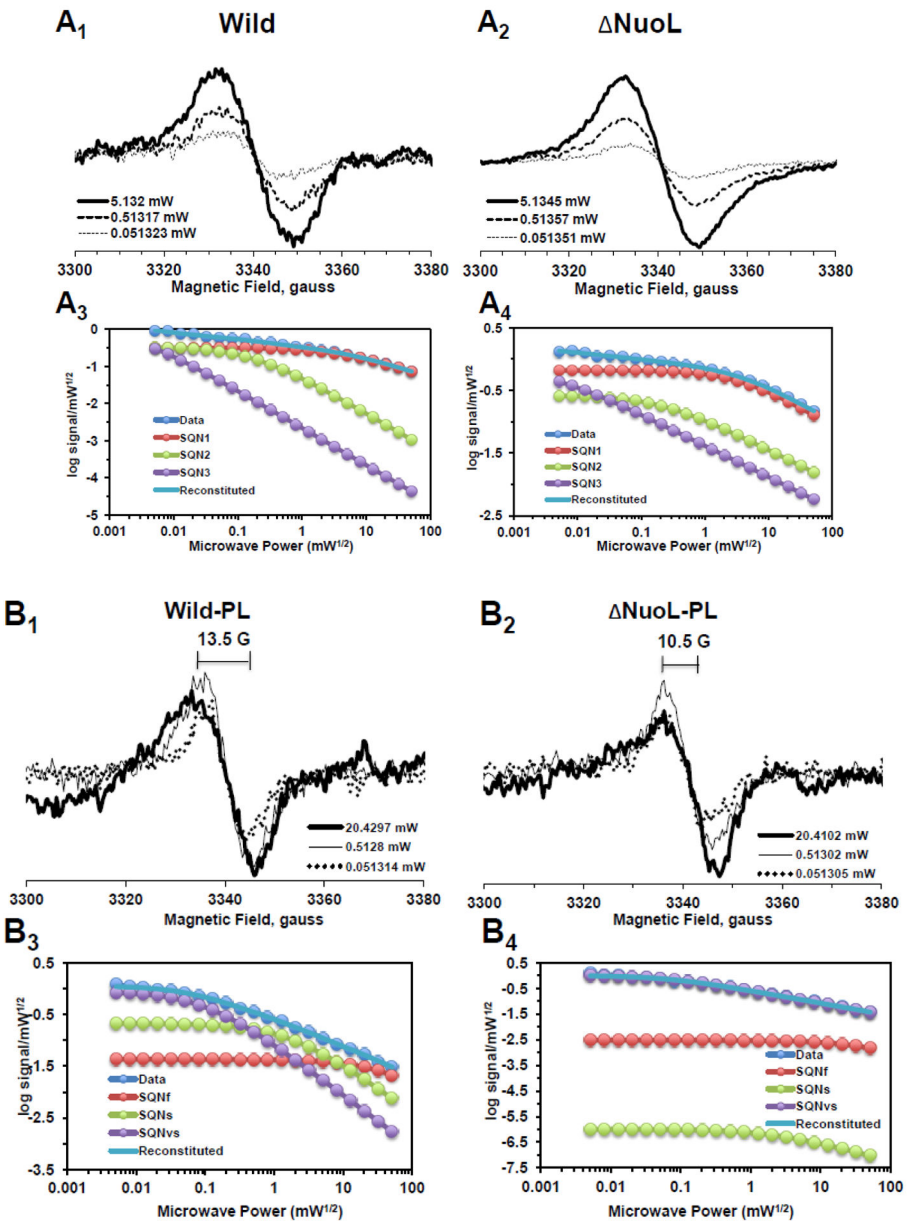

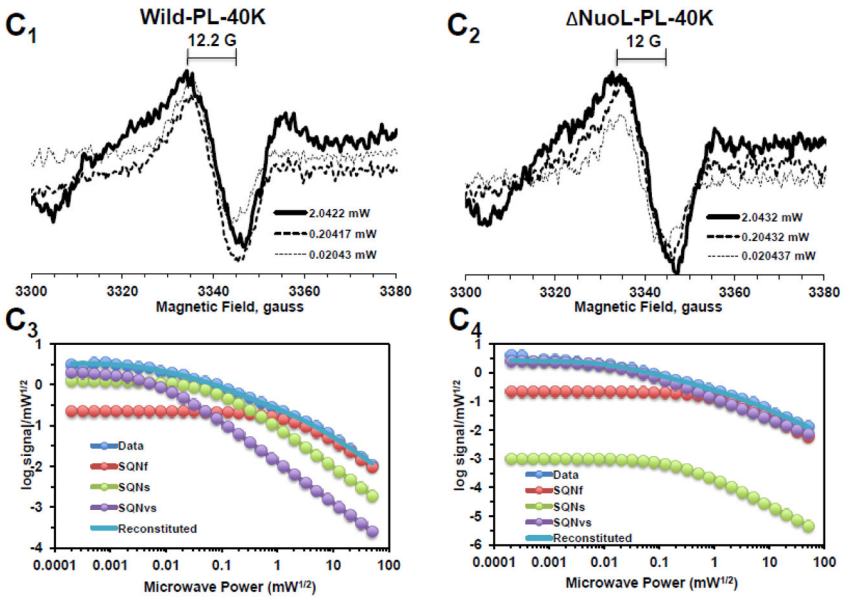

Fig. 2.

EPR spectra and the progressive power saturation profiles of ubisemiquinone g = 2.00 signals in the purified complex I at 150 K (A), the reconstituted complex I at 150 K (B) and 40 K (C). Panels A_1, B_1, and C_1, or A_2, B_2, and C_2 are EPR data for the wild-type or the ΔNuoL variant, respectively. A_3, B_3, and C_3, or A_4, B_4, and C_4, are the power saturation profiles of ubisemiquinones in the wild-type or the ΔNuoL variant, respectively. (A) The purified complex I (the wild-type, 8.28 mg/ml; the ΔNuoL variant,5.0 mg/ml) were anaerobically reduced with 6 mM NADH. The EPR data was analyzed as a three component system. “Data” and “Reconstituted” represent “actual EPR data” and “combined data of three resolved components after the fitting analysis”, respectively. The parameters obtained for the wild-type complex I are SQN1 (SQ species 1), C = 0.318; $P_{1/2}$ = 3.84; b = 1.104; SQN2 (SQ species 2): C= 0.335; $P_{1/2}$ = 0.164; b = 2; SQN3 (SQ species 3): C= 1.048; $P_{1/2}$ = 0.002; b = 2. The parameters obtained for the ΔNuoL variant are SQN1: C = 0.662; $P_{1/2}$ = 5.609; b = 1.211; SQN2: C= 0.261; $P_{1/2}$ = 0.292; b = 1; SQN3: C= 0.667; $P_{1/2}$ = 0.006; b = 1 (B) The reconstituted proteoliposomes were incubated on ice with 400 μM DQ, transferred into EPR tubes, and brought into an anaerobic chamber. The samples were anaerobically frozen at 10 sec after the addition of NADH to a final concentration of 2 mM. The parameters obtained for the wild-type are SQ_{Nf}: C = 0.0426; $P_{1/2}$ = 50; b = 2; SQ_{Ns}: C = 0.2118; $P_{1/2}$ = 1.624; b = 1.918; SQ_{Nvs}: C = 0.8782; $P_{1/2}$ = 0.1; b = 2. The parameters for the ΔNuoL variant are SQ_{Nf}: C = 0.0030; $P_{1/2}$ = 50; b = 2; SQ_{Ns}: C = 0.0000; $P_{1/2}$ = 2.0; b = 1.431; SQ_{Nvs}: C = 1.0163; $P_{1/2}$ = 0.1; b = 1. (C) The same proteoliposome samples described in (B) were used. The parameters for the wild-type are SQ_{Nf}: C = 0.2213; $P_{1/2}$ = 2.307; b = 2; SQ_{Ns}: C = 1.242; $P_{1/2}$ = 0.078; b = 2; SQ_{Nvs}: C = 2.0012; $P_{1/2}$ = 0.006; b = 2. The parameters for the ΔNuoL variant are SQ_{Nf}: C = 0.2135; $P_{1/2}$ = 1.405; b = 2; SQ_{Ns}: C = 0.001; $P_{1/2}$ = 0.229; b = 1.994; SQ_{Nvs}: C = 2.4572; $P_{1/2}$ = 0.017; b = 1.452. The g_z signal of cluster N1a signal, which partially overlaps with the SQ signals at high microwave powers, was subtracted using the corresponding data obtained from their counter samples that were anaerobically reduced with 20 mM dithionite. Other EPR conditions were: microwave

frequency, 9.45 GHz; modulation frequency, 100 kHz; modulation amplitude, 6 G; time constant, 82 ms. The concentrations and the specific activities of the proteoliposome samples are, Wild-type (WT)-proteoliposomes (PL): [1.8 mg/ml], NADH-DQ activity = 7.96 μmol/min/mg, NADH:ferricyanide activities = 78 μmol/min/mg; ΔNuoL-PL: [1.0 mg/ml], NADH-DQ activity = 2.38 μmol/min/mg, NADH:ferricyanide activities = 80.4 μmol/min/mg. The data shown in the figure are the representative data from three different samples for WT, WT-PL, and ΔNuoL-PL and two samples for ΔNuoL.

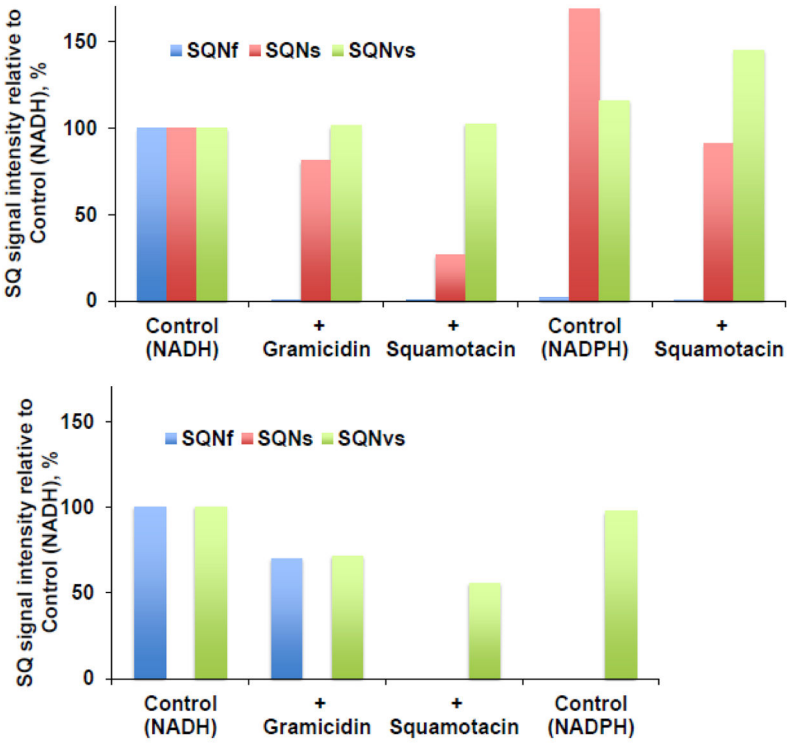

Fig. 3.

Effects of gramicidin D (an uncoupler, 100 μM), squamotacin (a potent complex I inhibitor, 100 μM), or NADPH (2 mM) on the ubisemiquinone g = 2.00 EPR signals in the wild-type complex I (A) and the ΔNuoL variant (B) reconstituted in proteoliposomes. SQ_{Nf} ($P_{1/2}$ = ~50 mW), SQ_{Ns} ($P_{1/2}$ = ~3 mW), and SQ_{Nvs} ($P_{1/2}$ = ~0.1 mW) were resolved by our computer fitting program. The data were obtained from the power saturation analysis at 51 mW for SQ_{Nf} (blue), 3 mW for SQ_{Ns} (red), and 0.08 mW for SQ_{Nvs} (green). The signal amplitudes of these SQ species (peak to peak) were measured. The EPR signal intensity was normalized relative to the control (NADH). There was no SQ_{Ns} ($P_{1/2}$ = ~3 mW) component in the ΔNuoL variant. [WT-PL] = 1.4 mg/ml, NADH:DQ= 14.19 μmol/min/mg and NADH:Ferricyanide = 132 μmol/min/mg. [ΔNuoL-PL] = 1 mg/ml, NADH:DQ= 2.38 μmol/min/mg and NADH:Ferricyanide = 80.4 μmol/min/mg. These are the representative data from two separate sets of samples.

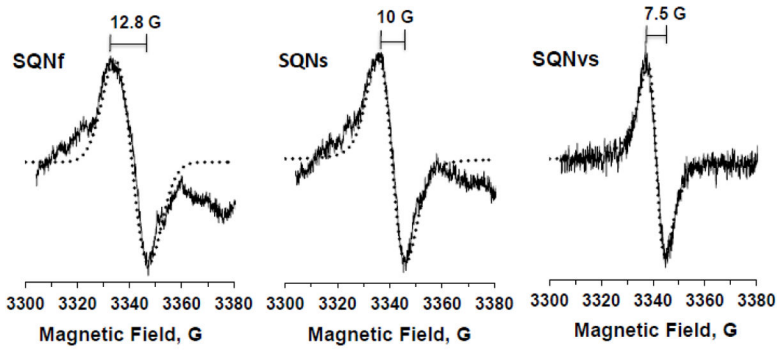

Fig. 4.

Three distinct SQ species in the wild-type complex I resolved by power saturation and simulation analyses. The SQ_{Nf} spectrum was obtained by subtracting 35% of SQ_{Ns} and 15% of SQ_{Nvs} from the control EPR data (reduced with NADH in the presence of DQ) at 20 mW. The SQ_{Ns} spectrum was obtained by subtracting 70% of SQ_{Nvs} from the EPR data reduced with NADH in the presence of DQ and gramicidin D at 3 mW. The SQ_{Nvs} spectrum was obtained from the EPR data reduced with NADH in the presence of DQ and squamotacin at 0.08 mW. The EPR conditions were the same as described in Fig. 2 except the data were accumulated 10 times. Simulated spectra are shown as dotted lines. The g-tensor principal values are: SQ_{Nf}, $g_x = 2.0046$, $g_y = 2.0067$, and $g_z = 2.0067$; SQ_{Ns}, $g_x = 2.0049$, $g_y = 2.0065$, and $g_z = 2.0065$; SQ_{Nvs}, $g_x = 2.0051$, $g_y = 2.0061$, and $g_z = 2.0061$. The ratios of Gaussian to Lorentzian broadenings are 1 to 0, 3 to 1, and 0 to 1 for SQ_{Nf}, SQ_{Ns}, and SQ_{Nvs}, respectively. The linewidths are shown in gauss.

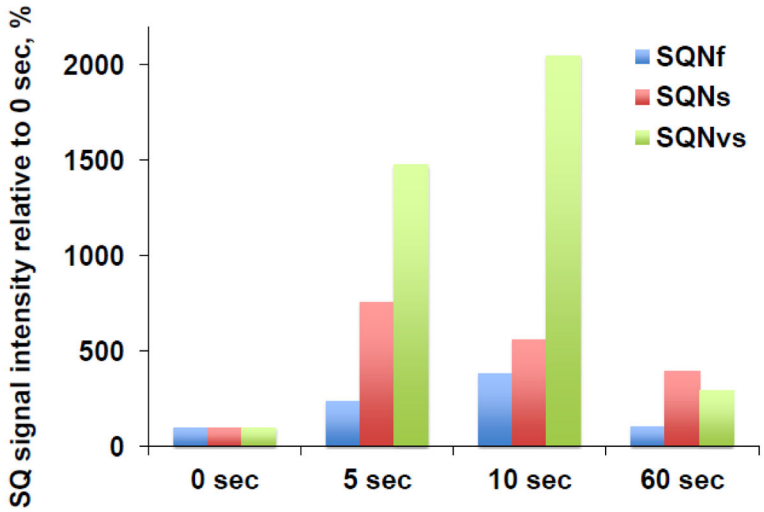

Fig. 5.

Time course of the SQ_{Nf}, SQ_{Ns}, and SQ_{Nvs} signals after the addition of NADH in the wild-type complex I reconstituted in proteoliposomes. The signal amplitude at 0 sec was determined from the EPR data for the sample in which only DQ was added (no NADH). Since the optimal microwave power to obtain the highest amplitude of each SQ species depends on microwave powers, the EPR data measured at 51 mW, 2 mW, and 0.2 mW were chosen to monitor the rise and decay time course of the SQ_{Nf}, SQ_{NS}, and SQ_{Nvs} signals, respectively. The total SQ signal intensity at 0 time was: 0.1197 at 51 mW; 0.0596 at 2 mW; 0.0452 at 0.2 mW. The changes in the intensity of each SQ signal are shown as % of the intensity at 0 time. [WT-PL] = 1.8 mg/ml, NADH:DQ = 7.96 μmol/min/mg and NADH:Ferricyanide = 78 μmol/min/mg. We measured three different sets of samples at 0 and 10 sec, two sets of samples at 0, 5, 10 sec, and two sets of samples at 0, 5, 10, and 60 sec.

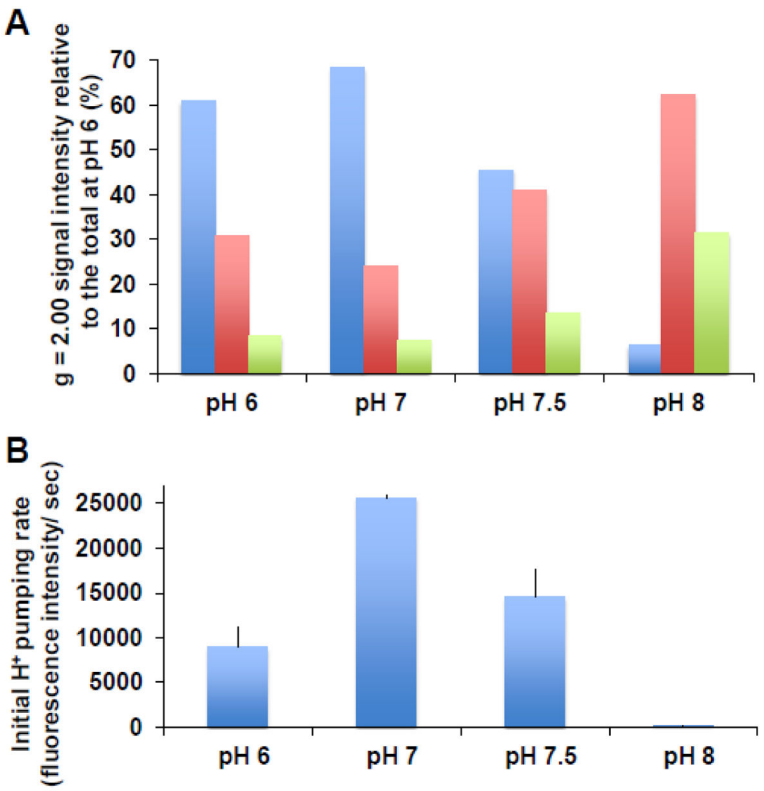

Fig. 6.

Effects of pH on the SQ_{Nf}, SQ_{Ns}, and SQ_{Nvs} signals (A) and the initial proton pumping rates (B). The signal amplitudes of SQ_{Nf}, SQ_{Ns}, and SQ_{Nvs} were normalized relative to the total SQ signals at pH 6, and they are shown in blue, red, and green bars, respectively. At the final washing step, suspended proteoliposomes were divided and separately collected in buffers at various pH as described in Experimental Procedures. The buffers used in enzyme assays were the same as buffers used for suspension of proteoliposomes at different pH. Both analyses were done with the same preparations. [WT-PL] = 1.91, 2.17, 1.86, and 1.87 mg/ml, NADH:DQ= 13.94, 9.16, 8.12, and 0.64 μmol/min/mg and NADH:Ferricyanide = 49.01, 40.87, 39.73, and 27.67 μmol/min/mg, at pH 6, 7, 7.5, and 8, respectively. Proton pumping activities were mean ± SD (n = 3, except for pH 8, n = 1).

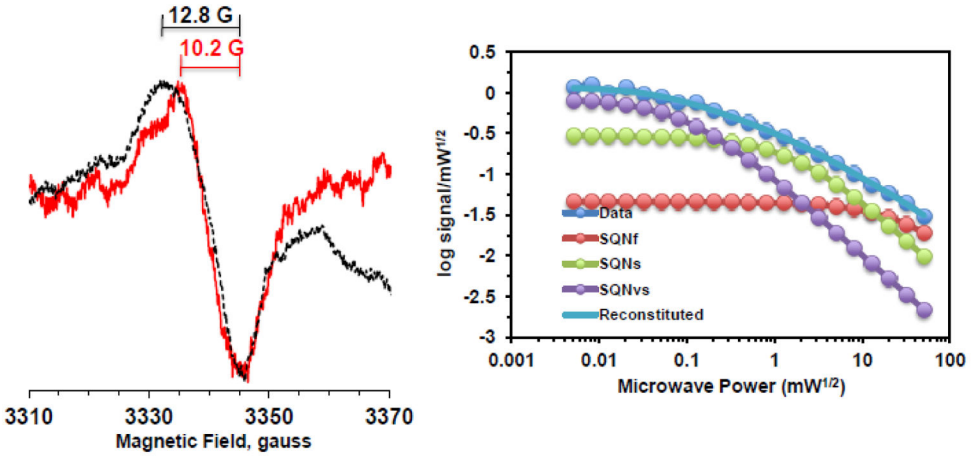

Fig. 7.

Effects of D_2O on SQ signals in the wild-type complex I reconstituted in proteoliposomes (1.68 mg/ml). *Left*, the EPR data at 20 mW and 150K from the samples prepared in H_2O and D_2O buffer were shown in black and red, respectively. *Right*, the progressive power saturation profiles of SQ signals in D_2O buffer. [WT-PL] in D_2O: 1.68 mg/ml, NADH:DQ = 8.98 μmol/min/mg and NADH:Ferricyanide = 49.28 μmol/min/mg.